Published in: Oristaglio, M. and Spies, B. (Eds.) "*Three-Dimensional Electromagnetics*", SEG (GD7), Tulsa, USA, 1999, 406-417.

Three-Dimensional Inversion of MT Fields Using Bayesian Statistics

Vjacheslav Spichak[1,2]

Michel Menvielle[2]

Michel Roussignol[3]

Summary. Bayesian statistics provide a formalism for inversion of magnetotelluric (MT) data in 3-D structures composed of elementary homogeneous domains. Available information (including assumptions about the model) is put in a probability density function (PDF) for *prior* values of the conductivities in the region of the search; the parameters to be found are the *posterior* values of the conductivity.

A stochastic algorithm called a Gibbs sampler estimates the posterior PDF. The outer cycle of the iterative inversion consists of scanning the homogeneous domains in the region of the search; the inner cycle involves solution of the forward problem for a set of models. This process represents a Markov chain, whose transition law converges to the marginal PDF of the parameters.

The inner cycle uses the finite-difference program FDM3D-MT, which computes electromagnetic responses in the frequency domain for 1-D, 2-D, or 3-D models. Iterative solution of the finite-difference equations is very fast and reduces greately the total CPU time since the results of the previous cycle are used as starting points for the next forward model. In most of our tests, the outer iteration converges in 15-20 iterations, which allows an attack on 3-D problems even on microcomputers. Examples show how the quantity and quality of data and the prior information affect the results of inversion.

1 Introduction

Inversion of magnetotelluric (MT) data aims to find a distribution of conductivity in the Earth that accounts for insufficient and noisy data, which often is spaced very irregularly on the surface. This ill-posed problem—whether solved stochastically or deterministically—requires regularization or the use of constraints. Questions about the existence and uniqueness of solutions become more critical for 3-D models with a large number of unknowns. Unfortunately, we do not know in advance how the

[1]Geophysical Research Center, Varshavskoe sh.8, Moscow 113105, Russia.
[2]Laboratoire de Physique de la Terre et des Planétes (URA 1369), Université Paris Sud, Bat. 504, 91405 ORSAY CEDEX, France.
[3]Equipe de Mathematiques Appliquées, Universite de Mame la Vallée, 2 rue de la Butte Verte, Noisy Ie Grand Cedex 93166, France.

data—the number of sites and their locations, the components of the electromagnetic (EM) field measured, the frequencies used, the noise, etc.—and the prior information available will affect the results of an inversion. It is thus not difficult to understand why inversions can give poor results. Attempts to improve the results usually involve increasing the volume of data or decreasing the number of parameters. This, in turn, can lead to overestimates of the amount of data needed to resolve the geoelectrical structure.

Despite some success with optimization methods for 3-D inversion of synthetic MT data (Mackie and Madden, 1993). inversion of real data will require careful attention to the issues mentioned above. Bayesian statistics provides an appropriate framework for studying these issues (see, e.g., Tarantola and Valette, 1982; Backus, 1988).

2 Bayesian inversion

In MT inversion, the conductivity model of the Earth can be divided into two kinds of regions: regions with known (or fixed) conductivity values and regions with (unknown) values to be determined by fitting the MT measurements at the Earth's surface, subject to contraints imposed by prior information. Each of the latter regions can be considered, in tum, as composed of homogeneous domains (cells). Let K be the total number of domains $\{P_k, k = 1,..., K\}$, whose conductivities $\sigma = (\sigma_k, k = 1, \ldots, K)$ are to be determined.

Let $\mathbf{E}(M_i, \omega_j, \sigma)$ be the electric field and $\mathbf{H}(M_i, \omega_j, \sigma)$ the magnetic field measured at given points (M_i ; i = 1,..., I}, on the Earth's surface for discrete frequencies $\{\omega_j;\ j = 1,..., J\}$. Also, let y_{ij} be values, derived from measurements, of a known function F(**E**, **H)** of these fields. The function F could be, for example, the impedance ratio of specific components of E and H. We assume that

$$y_{i,j} = F(\mathbf{E}(M_i, \omega_j, \sigma), \mathbf{H}(M_i, \omega_j, \sigma)) + \in_{i,j} \tag{1}$$

where $\{\in_{i,j}; i = 1, ..., I;\ j = 1, ..., J\}$ are noise functions, taken as realizations of independent random variables with probability density functions (PDFs) $p_{i,j}$ and zero-mean values.

An inversion for conductivity in the Earth usually involves simplifying assumptions (made from experience or convenience) about the regions of interest. The assumptions can be that the region is homogeneous, or that the conductivity variations are confined to a thin sheet, or are 1-D or 2-D in character. In the Bayesian approach, these prior assumptions and any prior knowledge are incorporated into the inversion through a probability law q, called the "prior PDF," on the set of possible values of the conductivities. The support of q (i.e, the set of ail possible values of conductivity) is the first choice to be made. Numerical computations make it necessary to define the support of q as a finite set. For simplicity, we suppose that thé number of possible conductivities consists of L different values $\{c_1,..., c_L\}$ for each homogeneous demain. The support of q is then the set A of the L^K possible elements (referred to below as images of the conductivity) $a = (a_k; k = 1, \ldots, K)$, where a_k belongs to $\{c_1,..., c_L\}$. The size of L determines the attainable precision of the inversion, and aiso the length of the computation (the search). We use the same set L of possible conductivities (called a "palette") for each domain, but it is possible to narrow the range of prior conductivities in some domain by setting appropriate prior probabilities equal to zero. If no information is available, it is still possible to limit the prior palette to lie between reasonable minimum and maximum values with a uniform PDF.

In the statistical point of view, both observations and model parameters (conductivities) are random variables. Our Bayesian analysis determines the posterior PDF of the conductivities—i.e., the conditional probabilities of the conductivities given the data y, prior information in terms of a conductivity palette (c_1,..., c_L) and PDF q, and the noise level ∈ .

$$P(\sigma = a / Y = y) = \frac{f(y/a)q(a)}{\sum_{b\in A} f(y/b)q(b)}, \tag{2}$$

where $q(a)$ is the prior probability of the image a and $f(y/a)$ is a conditional probability of the variable y = ($y_{i,j}$, i = 1,.../, j = 1,..., J) given the values of the conductivities. It is a function of a = (a_k, k = 1,..., K) through E and H and could be calculated directly as follows:

$$f(y/a) = \prod_{i=1}^{I}\prod_{j=1}^{J} p_{i,j}\left\{y_{i,j} - F\left[\mathbf{E}(M_i,\omega_j,a),\mathbf{H}(M_i,\omega_j,a)\right]\right\}, \tag{3}$$

where p_{ij} is the probability density of the noise ∈ $_{ij}$. If the probability densities $p_{i,j}$ are Gaussian with zero mean and covariances $(\zeta_{i,j})^2$, the above formula can be rewritten

$$f(y/a) = Z\exp(-\sum_{i,j}\frac{\left\{y_{i,j} - F\left[\mathbf{E}(M_i,\omega_j,a),\mathbf{H}(M_i,\omega_j,a)\right]\right\}^2}{2(\zeta_{i,j})^2}, \tag{4}$$

where Z is a normalizing constant. We assume the latter case, but note that the method presented also could be used without this assumption.

If $A(k, c_j)$ is a set of images that have the conductivity c_j, in the domain P_k, the kth marginal posterior probability p_k is

$$p_k(c_j) = P\left[\sigma \in A(k.c_j)/Y = y\right] = \frac{\sum_{a\in A(k,c_j)} f(y/a)q(a)}{\sum_{b\in A} f(y/b)q(b)}. \tag{5}$$

We can take as estimator of the conductivity in the domain P_k either the mean value the value corresponding to the maximum probability of the kth marginal posterior probability. However, in the above formula, there is a hidden difficulty: The denominator requires computation of $f(y/b)q(b)$ for all possible images b of the conductivity, or L^K times, which is unrealistic.

2.1 Markov chains

To overcome this difficulty we use a stochastic algorithm called a Gibbs sampler, which consists of an outer and an inner cycle. The outer cycle scans all K homogeneous domains in the regions of search; the inner cycle solves the forward problem for L prior values of the conductivity. Let [($\sigma_k^{(n)}$; k = 1,..., K] be the conductivities in the homogeneous domains in the regions of search after n iterations of the outer loop. If the domain $k(n)$ *is* scanned at iteration n+1, the image of conductivities is updated by changing only the conductivity of this domain to the new value chosen at random with the following probability:

$$P(\sigma_{k(n)}^{(n+1)} = c_j) = \frac{f(y/a(\sigma^{(n)},k(n),c_j))q(a(\sigma^{(n)},k(n),c_j))}{\sum_{j=1}^{L} f(y/a(\sigma^{(n)},k(n),c_j))q(a(\sigma^{(n)},k(n),c_j))} \tag{6}$$

where $a(\sigma, k, c_j)$ denotes the image equal to σ in all domains other than P_k, and equal to c_j in the domain P_k. Computation of P in equation (6) requires calculation of

$$f(y / a(\sigma^{(n)}, k(n), c_j)) q(a(\sigma^{(n)}, k(n), c_j))$$

L times. Thus, the total number of forward modelings per iteration of the outer cycle is just $L * K$.

The sequence of images $\left\lfloor \sigma^{(n)}, n \geq 0 \right\rfloor$ forms a random process, which is a Markov chain over the finite space of all possible images. The conditional probability, calculated in the kth domain at nth iteration is

$$po_k^n(c_j) = \frac{f(y / a(\sigma^{(k+nK)}, k, c_j)) q(a(\sigma^{(k+nK)}, k, c_j))}{\sum_{j=1}^{L} f(y / a(\sigma^{k+nK)}, k, c_j)) q(a(\sigma^{(k+nK)}, k, c_j))} \tag{7}$$

It can be proved that the posterior PDF is an invariant of this Markov chain and that, in each domain of the region of search, the sequence of the mean conditional probabilities converges toward the corresponding marginal probability,

$$p_k(c_j) = \lim_{N=\infty} \frac{1}{N+1} \sum p_k^n(c_j). \tag{8}$$

This gives an estimate of the mean posterior conductivities in each homogeneous domain of the region of search:

$$\sigma_k = \sum_{j=1}^{L} c_j po_k(c_j) \quad k = 1,..., K,$$

The solution of the inverse problem thus is reduced to the search for the a-posteriori conductivity distribution by means of successive solution of the forward problem for the prior values of the conductivities in the homogeneous domains.

2.2 Forward modeling

For forward modeling, we use the program FDM3D-MT (Spichak, 1983a), which has been checked against quasi-analytical solutions for a sphere buried in a free space (Spichak, 1983b) and against other numerical solutions (Zhdanov et al, 1990; Zhdanov and Spichak, 1992). The algorithm uses a seven-point finite-difference approximation of the integral "balance" equation for the electric field at each node of the grid. The system of sparse linear equations is solved by the block over-relaxation with adaptive correction of the relaxation factor. The vertical magnetic field is calculated from Maxwell's equation and the horizontal field by Hilbert transforms (see Spichak, 1999, this volume). The program is fast and allows calculation of the electromagnetic responses in the frequency domain in the earth or in the air for 1-D, 2-D, or 3-D structures with a relief surface.

3 Numerical experiments

We tested the Bayesian algorithm in numerical experiments with synthetic data. The model used for the synthetic data was a prism (1x1x1 km, 0.1 S/m), embedded at a depth 0.5 km in a halfspace of 0.01 S/m. With the two planes of symmetry, only one-quarter of the prism, discretized into 3 x 3 x4 cells (Fig. 1), was needed for numerical modeling. The data were values of the in-phase and quadrature electric-field

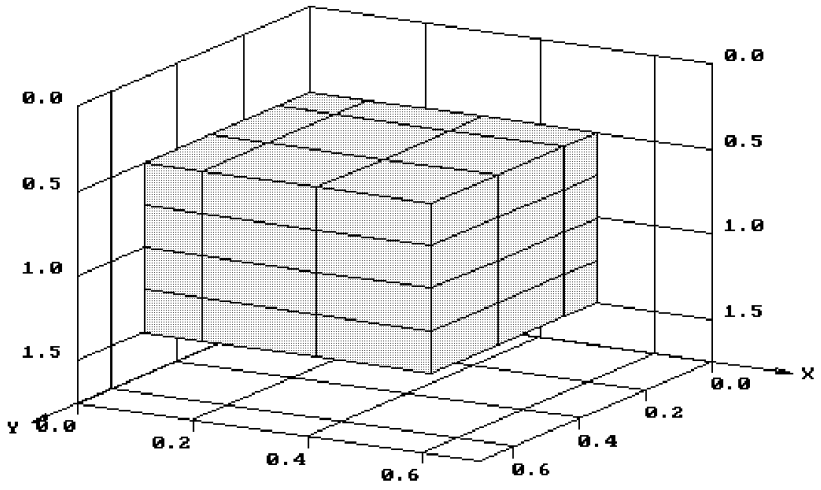

Figure 1. One-prism model used for generation of synthetic data.

components at 36 points at the Earth's surface for various periods and polarizations of the primary field.

To accelerate the inversion process we tried to use an approximate solution of the forward problem in the inner cycle of the inversion. We found, however, that this often led to bad values of conductivities in the domains scanned and could give an erroneous final conductivity distribution. So, to solve the forward problem accurately, we fixed the threshold for the rms error in the inner iteration process at the level 10^{-4}, which usually gave correct solutions of the forward problem. The inner iteration process converged in most cases in 20-50 iterations, depending on the a priori conductivity range preset, and the total CPU time required for one iteration of the outer cycle was quite reasonable.

Another important problem to solve was selection of an appropriate rule for stopping the outer iteration. The standard rule based on the misfit between the forward modeling results and the data is not suitable in our algorithm. In principle (statistically), more iterations of the outer cycle will always bring the result closer to the theoretical posterior conductivity distribution. On the other hand, we always have to settle for a finite number of iterations. The compromise found consists of stopping the iterations once the marginal mean posterior conductivities in the region of search are stabilized:

$$\left(\frac{1}{K} \sum_{k=1}^{K} \left(\frac{\sigma_k^{(n+1)} - \sigma_k^{(n)}}{\sigma_k^{(n)}} \right)^2 \right)^{1/2} < \in . \qquad (10)$$

Numerical experiments show that the level of 1 % for the left-hand side of this inequality is usually achieved in 15-20 iterations (Fig. 2).

The inversion code was tested on data synthesized for a false anomaly (with conductivity equal to those of the surrounding homogeneous half-space), which were inverted to search for the posterior conductivity distribution in the bounded region (Fig. 1) at periods T = 0.1,1,10,100, and 1000 s and for various prior conductivities ranging from 0.001 S/m to 0.1 S/m. Regardless of the prior PDF, the posterior mean conductivity in

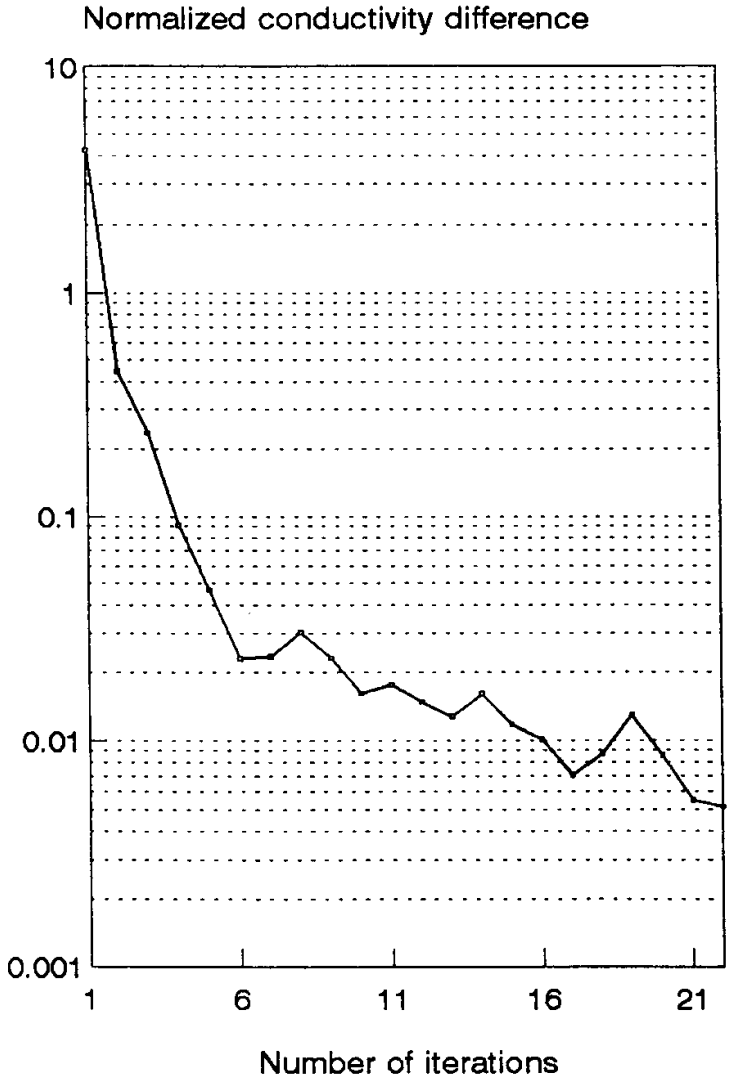

Figure 2. Normalized averaged conductivity difference as a function of iteration number for the model shown in Fig. 1.

the region of search practically coincided with the true value, or with the value from the prior conductivity range closest to the true one in cases when it was outside the prior palette.

3.1 Effect of prior conductivity palette

To study the effect of the prior conductivity palette and its range on the results of the inversion, we simulated two models with conductive (σ = 0.1 S/m) and resistive (σ = 0.001 S/m) prisms embedded in the homogeneous half-space (Fig. 1). The region of search coincided with the position of the prism so that the assumption about the homogeneity of the posterior conductivity distribution was valid. In the first experiment, the prior conductivity palette ranged from 0.01 S/m to 0.1 S/m for the conductive target and from 0.001 S/m to 0.01 S/m for the resistive one. In the second experiment, the range (and, correspondingly, the sampling) was increased 10 times—from 0.001 S/m to 0.1 S/m—for both conductive and resistive prisms (with a uniform PDF). The results of the inversion showed that the conductivities of the targets could be reconstructed with

accuracy 4% for conductive body and with accuracy 20% for resistive body regardless of the prior conductivity range and the periods used.

3.2 Relative importance of prior information and data

Another experiment was carried out to study the relative importance of the prior PDF and the data. As in the previous experiment, reconstructions of two different target conductivities were made from the synthetic electric-field components for the periods 1 s and 10 s. The prior conductivities were 0.1 S/m and 0.01 S/m in the case of the conductive body and 0.001 S/m and 0.01 S/m in the case of the resisitive one. Standard deviations of the noise added to synthetic data were 3%, 5%, and 10%. For each input data set and each level of noise, the prior PDF was changed so that the probability attributed to the conductivity that was equal to the true target conductivity ranged from 0.1 to 1.0.

The results of the experiments indicate that, up to a 5% level of noise, the prior PDF has no effect on the posterior one in either case. When the level of the noise increases to 10%, however, the reconstruction of the resistive target becomes sensitive to the prior PDF; reconstruction of the conductive target remains stable. Figure 3 shows the graphs of the posterior mean conductivity, normalized by the true value in the case of reconstruction of the resistive body for the periods 1 s and 10 s. (The straight line denotes a normalized mean prior value of the target conductivity, based on the prior palette and PDF.) Figure 3 shows that, in the worst case, when the prior probability that the target conductivity equals the true conductivity is only 0.1, the posterior conductivity can be overestimated by a factor of two or even three, depending on the period of the input data. The differences between the straight and the curved lines can be interpreted as the contribution of the input data to the inversion: The more accurate the prior estimation of the target conductivity, the less important is the contribution of the input data (and vice versa). Figure 3 illustrates this effect quantitatively.

Another useful characteristic of the Bayesian inversion is the statistical uncertainty of the posterior values of the parameters. Nonuniqueness of the inversion can be measured by the standard deviations of the posterior conductivities. Figure 4 shows the graph of the posterior normalized mean conductivity as the prior probability of the target conductivity coinciding with the true value varies, for the case of the resistive prism (period T = 1 s, Gaussian noise 10% is added to synthetic data). The uncertainty of the result decreases when the prior estimates of the target conductivity become closer to their true values.

3.3 Effect of data

Some experiments were done to study the influence of the structure and the volume of the input data on the results of the inversion. Here we describe only one result, which is important for understanding the mechanism of the inversion. Synthetic electric-field components were generated for conductive and resistive prisms of the same geometry (Fig. 1) at the period 10 s and inverted using only one polarization of the primary field (along the x-axis). Each cell of the grid was considered as a homogeneous domain in the region of search. Figure 5 shows the results of the inversions after 15 iterations for conductive ((a) and (b)) and resistive ((c) and (d)) targets. With a conductive anomaly, the conductivities are reconstructed with the relative error up to 9% in the

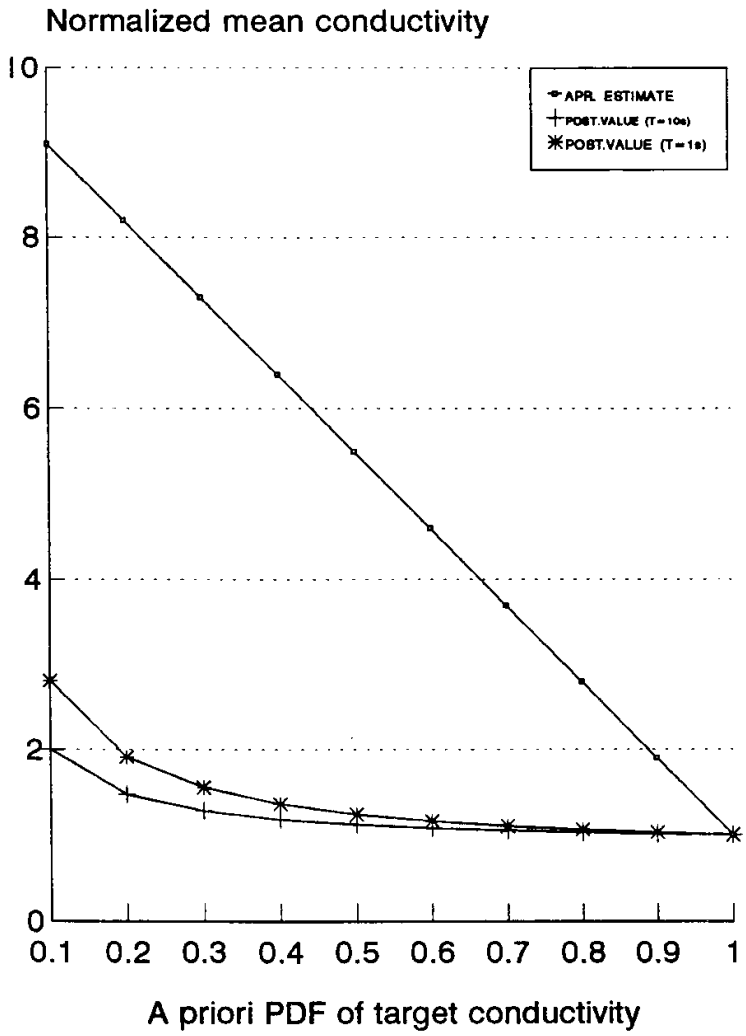

Figure 3. Relative contribution of prior PDF estimation and data to results of inversion for the model shown in Fig. 1; 10% Gaussian noise is added to synthetic data.

region with dimensions 0.3 x 0.3 x 0.7 km (25% of the volume of the region of search), whereas with a resistive anomaly, the values in the same region are reconstructed with the relative error up to 90%.

There is also a different accuracy of the conductivity reconstruction at the boundaries parallel and perpendicular to the direction of the primary field polarization. With a conductive anomaly, the best results are achieved at the parallel boundaries (TE mode) (Fig. 5b), whereas with a resistive anomaly, the results are evidently better at perpendicular boundaries (TM mode) (Fig. 5c). We believe that these results are caused by different mechanisms dominating in the inversion when a conductive or a resistive prior conductivity palette is used. Indeed, because of galvanic effects, the electric field in both cases is sensitive to the perpendicular boundaries; however, because of inductive effects, the electric field becomes sensitive to parallel boundaries only with conductive regions in the palette. Thus, when using the electric fields for the inversion, it is important to match in advance the prior conductivity palette and the range of periods used to get accurate results in a minimum number of iterations.

In another experiment, the volume of data was increased 4 times. The data consisted of synthetic electric fields mixed with 1% Gaussian noise for two polarizations of the

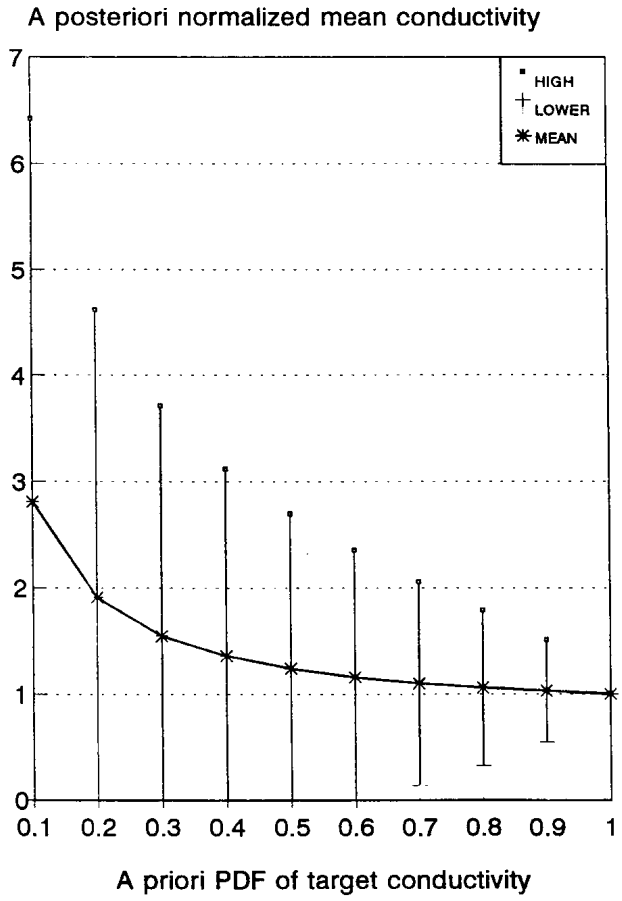

Figure 4. Effect of prior PDF on the uncertainty in posterior conductivity estimation for model shown in Fig. 1. Period T = 1 s; 10% Gaussian noise is added to synthetic data.

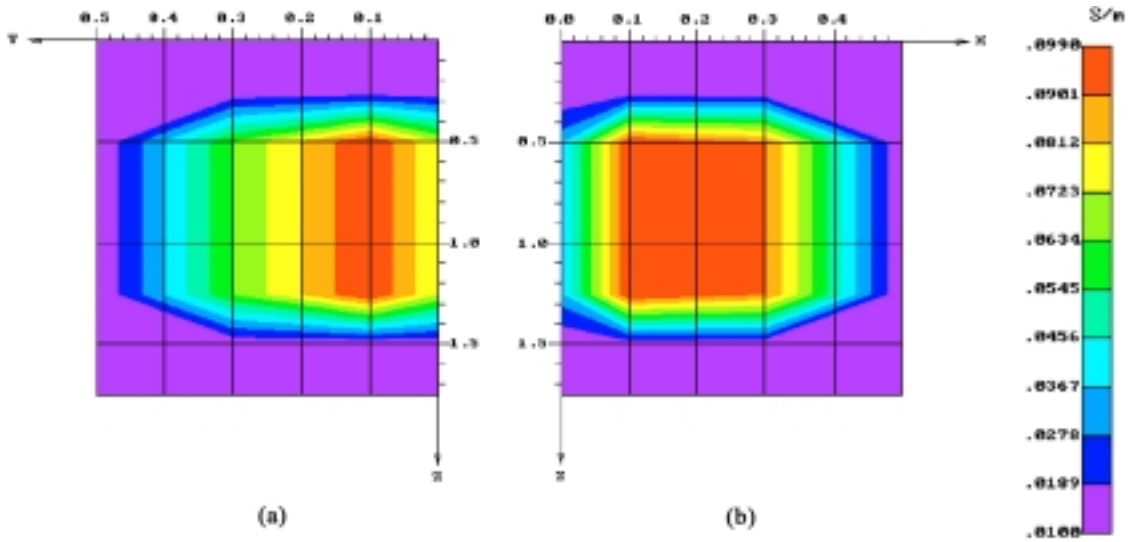

Figure 5. Resolution of conductive ((a) and (b)) and resistive ((c) and (d)) prisms shown in Fig. 1, embedded in the homogeneous half-space (σ = 0.01 S/m): (a,c) *yz* cross-sections (*x* = 0.3 km); (b,d) *xz* cross-sections (*y* = 0.3 km). Data inverted: Synthetic electrical field components, mixed with 1% Gaussian noise; primary field is polarized in *x*-axis, T = 10 s. Prior information used: σ_1^c =0.01 S/m, σ_2^c = 0.055 S/m, σ_3^c = 0.1 S/m; σ_1^r = 0.0 S/m, σ_2^r = 0.003 S/m, σ_3^r =0.00 S/m; p_i = 0.333, p_2. = 0.333, p_3 = 0.333.

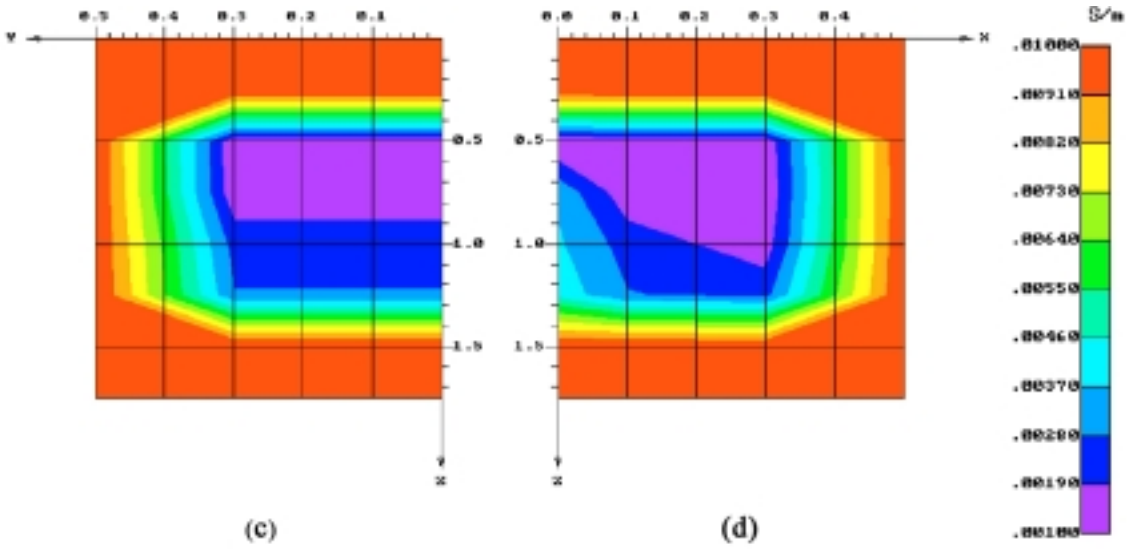

Figure 5. (*Continued*)

PLANE VIEW

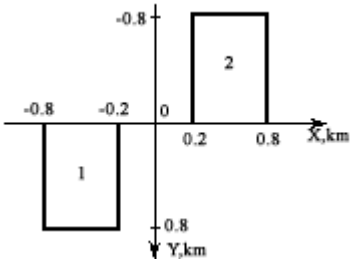

CROSS SECTION

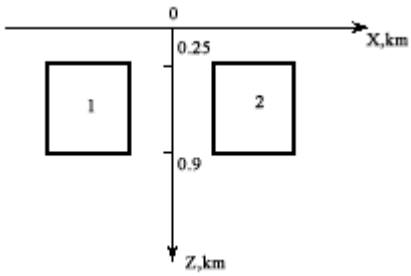

Figure 6.

primary field at two periods (T = 1, 10s). A two-prism model consisting of conductive (1) and resistive (2) prisms, buried in the homogeneous half-space was used for generation of synthetic data (Fig. 6). The conductivities of the targets were 0.1 S/m and 0.001 S/m, correspondingly, and the conductivity of the homogeneous half-space was equal to 0.01 S/m.

The region of search consisted from 5 x 5 x 7(=175) cells and ranged from —1.0 km to 1.0 km along each horizontal coordinate axis and from the earth surface to the depth2

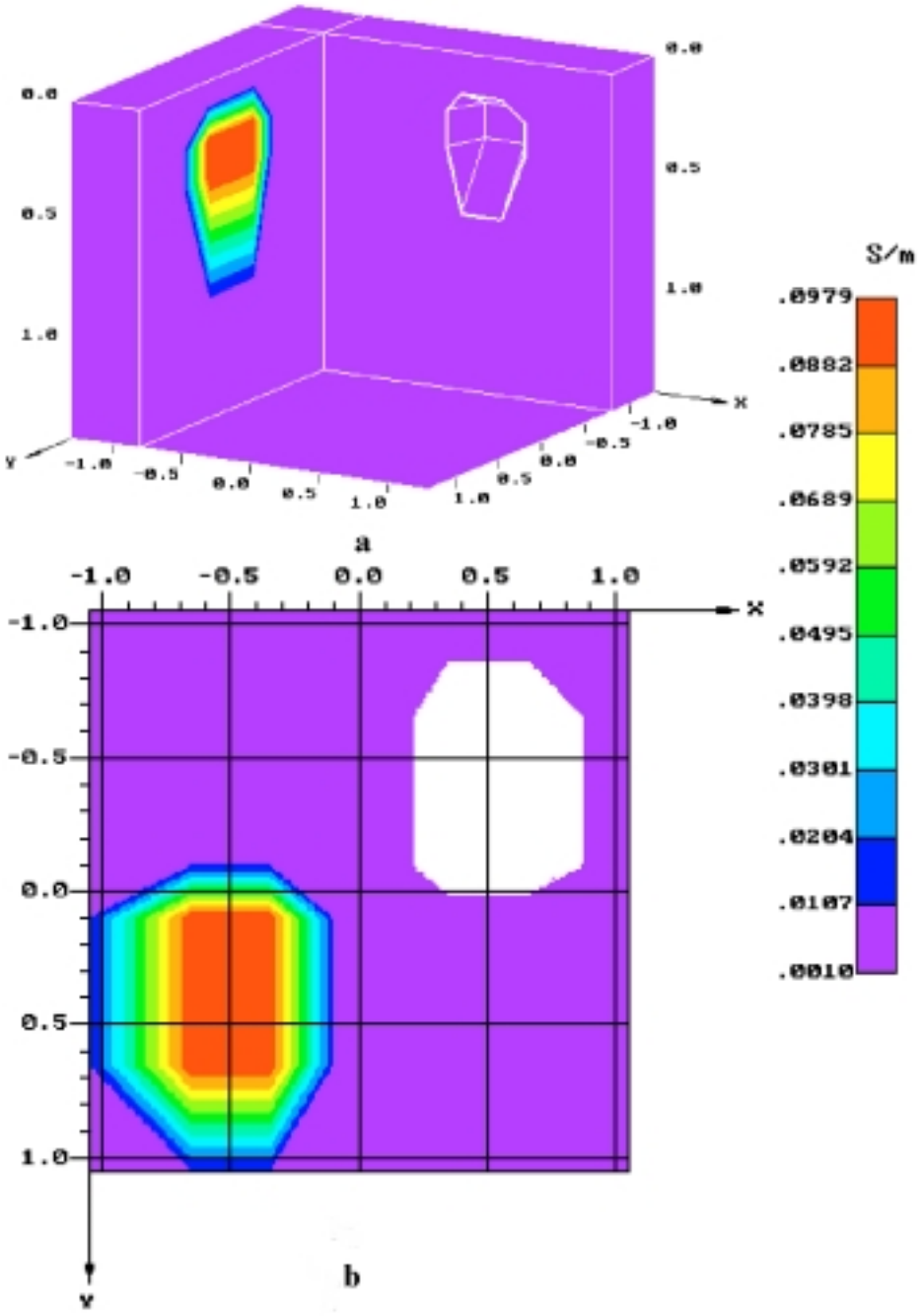

Figure 7.

km. The prior conductivity palette ranged from σ_{min} = 0.001 S/m to (σ_{max} =0.1 S/m with sampling 0.1 (σ_{max} — σ_{min}) and uniform PDF.

Figure 7(a, b) shows the result of the inversion. The posterior conductivity values in the domains occupied by prisms differ from the model ones by not more than 7% for conductive prism and by 45% for resistive one. The comparison of these results with the previous ones clearly indicates the effect of the volume of data used for inversion.

Comparison of these results with those discussed in the Section 3.1 (inversions for conductive and resistive prisms separately) suggests that the additional hypothesis that the region of search consists only of domains occupied by homogeneous prisms would result in improvement of the accuracy of reconstruction, especially in the case of a resistive target (from 45% to 20%).

4 Conclusions

A Bayesian approach has proved to be an efficient tool for 3-D inversion of MT data. It incorporates the prior information into the inversion procedure in a flexible way and converts the problem of nonuniqueness to the practical task of estimating posterior uncertainties. Results of synthetic experiments show that 3-D inversion can be done in a reasonable time on a PC 486. However, to use this method for inversion of real data, we need to accelerate even more the iterations and devise better interpretation strategies for different types of input data.

Acknowledgments

This work was made in the frames of P.A.S.T. position of one of the authors (V. Spichak) at the Universite Paris Sud (Laboratoire de Physique de la Terre et des Planetes). The authors wish to thank the anonymous referees and the editors for their valuable suggestions and comments.

References

Backus, G. E., 1988, Bayesian inference in geomagnetism: Geophys. J., **92,** 125-142.

Geman**,** S., and Geman, D., 1984, Stochastic relaxation, Gibbs distribution, and the Bayesian restoration of images; IEEE Trans. Pattern Analysis and Machine Intelligence, **6**, 721-741.

Grandis, H**.,** 1994, Imagerie électromagnétique Bayesienne par la simulation d'une chaine de Markov: Doctoral d'Université, Université Paris VII.

Jouanne, V., 1991, Application des techniques statistiques Bayesiennes `a 1'inversion de données électromagnétiques: Doctoral d'Université, Université Paris VII.

Mackie, R. L., and Madden, T. R,, 1993, Three-dimensional magnetotelluric inversion using conjugate gradients: Geophys. J. Internat., **115,** 215-229.

Press, S. J., 1989, Bayesian statistics: principle, models and applications: John Wiley & Sons.

Roussignol, M., Jouanne, V., Menvielle, M., and Tarits, P., 1993, Bayesian electromagnetic imaging: in Hardle, W., and Siman, L., Eds., Computer intensive methods, Physical Verlag, 85-97.

Spichak, V., 1983a, The FDM3D program package for numerical modeling of the three-dimensional electromagnetic fields: in Algorithms and programs for solution of the direct and inverse problems of electromagnetic induction in the Earth, Ed, Zhdanov, M. S., 1ZMIRAN Publ, 58-68 (in Russian).

Spichak, V., 1983b, Mathematical modeling of EM fields in 3D inhomogeneous media:

Ph.D. Thesis, 1ZMIRAN, 215 (in Russian).

Tarantola, A., and Valette, B., 1982, Inverse problems: Quest for information: J. Geophys., **50,** 159-170.

Zhdanov, M., Varentsov, Iv., Golubev, N., and Krilov, V., 1990, Methods of modeling of the EM fields: Nauka PubL, 200 (in Russian).

Zhdanov, M.**,** and Spichak V., 1992, Mathematical modeling of EM fields in 3-D inhomogeneous media: Nauka Publ, 188 (in Russian).